

## LYMPHOID NEOPLASIA

Ibrutinib inhibits pre-BCR<sup>+</sup> B-cell acute lymphoblastic leukemia progression by targeting BTK and BLK

Ekaterina Kim,<sup>1</sup> Christian Hurtz,<sup>2,3</sup> Stefan Koehrer,<sup>1,4</sup> Zhiqiang Wang,<sup>5</sup> Sriram Balasubramanian,<sup>6</sup> Betty Y. Chang,<sup>7</sup> Markus Müschen,<sup>2</sup> R. Eric Davis,<sup>5</sup> and Jan A. Burger<sup>1</sup>

<sup>1</sup>Department of Leukemia, University of Texas MD Anderson Cancer Center, Houston, TX; <sup>2</sup>Department of Laboratory Medicine, University of California San Francisco, San Francisco, CA; <sup>3</sup>Division of Hematology and Oncology, Department of Medicine, University of Pennsylvania, Philadelphia, PA; <sup>4</sup>Department of Pediatrics and Adolescent Medicine, Ulm University Medical Center, Ulm, Germany; <sup>5</sup>Department of Lymphoma/Myeloma, University of Texas MD Anderson Cancer Center, Houston, TX; <sup>6</sup>Janssen Research & Development, LLC, Springhouse, PA; <sup>7</sup>Pharmacyclics, Inc., Sunnyvale, CA

## Key Points

- In B-ALL, cells that express a functional pre-BCR ibrutinib abrogate leukemia cell growth in vitro and in vivo.
- Effects of ibrutinib in B-ALL not only are mediated through inhibition of BTK but also involve BLK inhibition.

Targeting B-cell receptor (BCR) signaling is a successful therapeutic strategy in mature B-cell malignancies. Precursor BCR (pre-BCR) signaling, which is critical during normal B lymphopoiesis, also plays an important role in pre-BCR<sup>+</sup> B cell acute lymphoblastic leukemia (B-ALL). Here, we investigated the activity and mechanism of action of the BTK inhibitor ibrutinib in preclinical models of B-ALL. Pre-BCR<sup>+</sup> ALL cells were exquisitely sensitive to ibrutinib at therapeutically relevant drug concentrations. In pre-BCR<sup>+</sup> ALL, ibrutinib thwarted autonomous and induced pre-BCR signaling, resulting in deactivation of PI3K/Akt signaling. Ibrutinib modulated the expression of pre-BCR regulators (PTPN6, CD22, CD72, and PKC $\beta$ ) and substantially reduced BCL6 levels. Ibrutinib inhibited ALL cell migration toward CXCL12 and beneath marrow stromal cells and reduced CD44 expression. CRISPR-Cas9 gene editing revealed that both BTK and B lymphocyte kinase (BLK) are relevant targets of ibrutinib in pre-BCR<sup>+</sup> ALL. Consequently, in mouse

xenograft models of pre-BCR<sup>+</sup> ALL, ibrutinib treatment significantly prolonged survival. Combination treatment of ibrutinib with dexamethasone or vincristine demonstrated synergistic activity against pre-BCR<sup>+</sup> ALL. These data corroborate ibrutinib as a promising targeted agent for pre-BCR<sup>+</sup> ALL and highlight the importance of ibrutinib effects on alternative kinase targets. (*Blood*. 2017;129(9):1155-1165)

## Introduction

B-cell acute lymphoblastic leukemia (B-ALL) is a B lymphocyte progenitor malignancy that arises predominantly during childhood,<sup>1,2</sup> with a second peak in incidence after the age of 50 years.<sup>3</sup> Outcome for pediatric patients is fairly good, with 5-year event-free survival rates above 80%; in contrast, the outcome in adult patients generally is less favorable. The introduction of kinase inhibitors targeting B-cell receptor (BCR) signaling generated hope that these compounds may become useful for the treatment of various B-cell malignancies, especially those that depend upon BCR signaling.<sup>4,5</sup> Signaling of the precursor B-cell receptor (pre-BCR) is largely similar to that of the mature BCR and plays a critical role during early B-cell development.<sup>6</sup> In the bone marrow, the pre-BCR promotes survival and expansion of progenitor cells with productively rearranged pre-BCRs, and B-cell precursors with non-functional pre-BCRs are targeted for deletion. During normal B-cell development, pre-BCRs are expressed for a short period of time after successful immunoglobulin heavy chain (*IGH*) gene rearrangement, allowing progenitor cells to transition into the pool of mature peripheral B cells. Pre-BCR surface levels are lower than those of the mature BCR,

presumably due to continuous activation and receptor internalization.<sup>7</sup> Different mechanisms of pre-BCR activation have been described. Several lines of evidence demonstrated ligand-independent autonomous (tonic) pre-BCR activation via self-aggregation being a central mechanism,<sup>6,8-10</sup> whereas other studies suggested a role of stromal cell antigens, such as galectin-1, as candidate ligands of the pre-BCR.<sup>11</sup>

The role of pre-BCR signaling in ALL may differ depending on the maturation stage of the lymphoblasts and presence of oncogenic driver lesions. For instance, pre-BCR signaling is compromised in most BCR-ABL1<sup>+</sup> cases of ALL through nonproductive *IGH* gene rearrangement or deregulation of other pathway components, such as IKAROS, SLP-65, and Bruton tyrosine kinase (BTK).<sup>12-15</sup> BCR-ABL1<sup>+</sup> and cytokine receptor/STAT5-driven ALL cells are preferentially selected against subclones with functional pre-BCRs, because in these ALL subtypes the pre-BCR suppresses rather than promotes proliferation of the leukemia cells.<sup>16,17</sup> In contrast, a subset of ALL cases, including over 90% of the cases carrying translocation (1;19), have productively rearranged *IGH* genes and rely on pre-BCR-dependent Akt activation

Submitted 16 June 2016; accepted 19 December 2016. Prepublished online as *Blood* First Edition paper, 28 December 2016; DOI 10.1182/blood-2016-06-722900.

Presented, in part, at the 54th annual meeting of the American Society of Hematology, Atlanta, GA, 8-11 December 2012, and at the 55th annual meeting of the American Society of Hematology, New Orleans, LA, 7-10 December 2013.

The online version of the article contains a data supplement.

There is an Inside *Blood* Commentary on this article in this issue.

The publication costs of this article were defrayed in part by page charge payment. Therefore, and solely to indicate this fact, this article is hereby marked "advertisement" in accordance with 18 USC section 1734.

© 2017 by The American Society of Hematology

for their proliferation.<sup>18,19</sup> Pre-BCR-dependent ALL accounts for approximately 15% of ALL cases and was recently shown to be exquisitely sensitive to BCR signaling inhibitors.<sup>17,20</sup>

BTK is a tyrosine kinase downstream of the pre-BCR and BCR and is present in normal B cells at all stages of maturation, except in plasma cells.<sup>21-23</sup> BTK transduces signals that foster B-cell differentiation, proliferation, survival, and tissue homing.<sup>24,26</sup> The importance of BTK in the pathogenesis of chronic lymphocytic leukemia, diffuse large B-cell lymphoma, and other mature B-cell malignancies is well established,<sup>27-29</sup> but there is less information about BTK's role in ALL. Early studies reported unaltered levels of BTK in childhood ALL cells,<sup>30</sup> whereas frequent BTK deficiency due to aberrant splicing was reported later.<sup>31,32</sup> Ibrutinib was recently suggested as a potential therapeutic option for pre-BCR<sup>+</sup> or *TCF3*-rearranged ALL.<sup>17,33</sup> However, another study reported that t(1;19)-ALL is sensitive to the SRC/ABL/BTK inhibitor dasatinib but not to ibrutinib or BTK knockdown.<sup>19</sup> Here, we explore the preclinical therapeutic potential of ibrutinib in ALL and mechanism of its action. We provide evidence that ibrutinib interferes with pre-BCR signaling and suppresses ALL cell proliferation, acting through multiple targets, especially BTK and BLK tyrosine kinases. Ibrutinib significantly prolonged survival in a mouse model of human pre-BCR<sup>+</sup> ALL.

## Materials and methods

### Patient samples and cell lines

Cell lines were validated by short tandem repeat (STR) method and assigned to various immunophenotypes on the basis of immunoglobulin heavy and light chain expression; immunoglobulin  $\mu$ -chain<sup>-</sup> (Ig $\mu$ <sup>-</sup>) defined a pro-B cell, Ig $\mu$ <sup>+</sup> a pre-B cell, and IgM<sup>+</sup> a mature B-cell phenotype of the ALL cells.

After informed consent obtained in accordance with the Declaration of Helsinki on protocols reviewed and approved by the institutional review board at the MD Anderson Cancer Center, peripheral blood samples were drawn from patients fulfilling clinical and immunophenotypic criteria for B-ALL at the Department of Leukemia, MD Anderson Cancer Center. Peripheral blood mononuclear cells were maintained in coculture with KUSA-H1 murine stromal cells in RPMI 1640 medium, supplemented with 10% fetal bovine serum (Gibco), 2.05 mM of L-glutamine (HyClone Laboratories), and penicillin-streptomycin (Corning).

### Cell counting and viability assay

Staining with 3,3 dihexyloxocarbocyanine iodide (DiOC6; Molecular Probes) and propidium iodide (PI; Molecular Probes) was used to measure the percentage of viable cells, as has been previously described.<sup>34</sup> Primary ALL samples were considered only if the viability of untreated cells was over 55% after 48 hours of *ex vivo* culture. Relative cell numbers were determined by counting at high flow for 20 seconds, or absolute cell numbers were measured with CountBright Absolute Counting Beads (Molecular Probes).

### Western blot

In this study we used antibodies against the following proteins: pBTK-Y223 (Epitomics, Abcam), BTK, p-phospholipase C (pPLC) $\gamma$ 2, PLC $\gamma$ 2, p-protein kinase B (Akt)-S473, pAkt-T308, Akt, p-extracellular signal-regulated kinase (pERK)1/2-T202/Y204, ERK1/2, BCL6, SHP-1 (PTPN6), pS6-S235/236, S6, glyceraldehyde-3-phosphate dehydrogenase (GAPDH), pFOXO1-Thr24/FOXO3a-Thr32/FOXO4-Thr28, FOXO1, FOXO3a, FOXO4, p27, and BLK (Cell Signaling). Densitometry analysis was performed using ImageJ software.

### XTT proliferation assay

Cell proliferation was measured using TACS XTT Cell Proliferation/Viability Assay (Trevigen), according to the manufacturer's instructions. Half-maximal inhibitory concentrations (IC<sub>50</sub>) were calculated using Prism 6 for Mac OS X

(GraphPad Software; <http://www.graphpad.com>). Cells were incubated with increasing concentrations of ibrutinib for 72 hours (cell lines) or 96 hours (*BLK/BTK* KO cells). Combination experiments were analyzed with CompuSyn (ComboSyn Incorporated; <http://www.combosyn.com/>).

### Measurement of intracellular calcium mobilization

Calcium mobilization was measured, as has been described previously.<sup>35</sup> ALL cells were loaded with Fluo-3 AM (Invitrogen) and Pluronic F-127 (Sigma-Aldrich) and then treated with 0.1% dimethyl sulfoxide (DMSO) or 1  $\mu$ M of ibrutinib for 30 minutes. Calcium mobilization was induced by 10  $\mu$ g/mL of the goat F(AB')<sub>2</sub> fragment to human IgM (MP Biomedicals). Fluorescence was measured with flow cytometry. The data were analyzed using FlowJo (version 9.4.11; FlowJo; <http://www.flowjo.com/>).

### Flow cytometry

Flow cytometry analyses were performed on a BD FACSCalibur (BD Biosciences). The following monoclonal antibodies were used in accordance with the manufacturer's instructions: CD22-phycoerythrin (PE), CD72-fluorescein isothiocyanate (FITC), and CD44-FITC (BD Biosciences).

### Gene expression profiling

Total RNA was isolated from RCH-ACV cells treated with 0.1% DMSO or 1  $\mu$ M of ibrutinib for 24–72 hours using TRIzol Reagent (Ambion) and RNeasy Mini Kit (QIAGEN). After confirming RNA quality with a Bioanalyzer 2100 instrument (Agilent), 300 ng of total RNA was amplified and biotin-labeled through an Eberwine procedure using an Illumina TotalPrep RNA Amplification kit (Ambion) and hybridized to Illumina HT12 version 4 human whole-genome arrays. Data were processed, as has been described previously.<sup>36</sup> Hierarchical clustering with the Average linkage clustering method was performed with Cluster 3.0 (Human Genome Center, University of Tokyo, Tokyo, Japan). Resulting data were analyzed using QIAGEN's Ingenuity Pathway Analysis ([www.ingenuity.com](http://www.ingenuity.com)). The St. Jude B-ALL GEP dataset (GSE33315)<sup>37</sup> was downloaded from the National Center for Biotechnology Information gene expression omnibus gene expression database (<http://www.ncbi.nlm.nih.gov/geo/>) and analyzed by applying the Gene Pattern Server provided by the Broad Institute (Cambridge, MA), as has been previously described.<sup>20</sup>

### Chemotaxis assay and migration assay (pseudoeemperipolesis)

Chemotaxis of control or ibrutinib-treated (0.5  $\mu$ M, 1 hour) cells toward CXCL12 (100 ng/mL; R&D Systems) was performed, as has been previously described, using 6.5-mm Transwell culture inserts (Costar) with a pore size of 5 or 8  $\mu$ m.<sup>38</sup>

Migration assay was performed, as has been described previously.<sup>38</sup> KUSA-H1 cells were plated in collagen-coated 12-well plates 24 hours before the experiment ( $1.4 \times 10^5$  per well). ALL cells were pretreated with 0.1% DMSO or 0.5  $\mu$ M ibrutinib for 72 hours. We layered  $5 \times 10^6$  ALL cells on top of the stromal cells for 4 hours.

### Mouse model of human ALL

The ICN12<sup>17</sup> human ALL model experiment was in compliance with the institutional approval by the University of California, San Francisco. ICN12 cells were labeled with lentiviral firefly luciferase, and  $1 \times 10^6$  cells were injected via tail vein into 14 sublethally irradiated nonobese diabetic (NOD)/severe combined immunodeficiency (SCID) recipient mice (7 per group). Engraftment and leukemia expansion were monitored by using luciferase bioimaging. Ibrutinib was administered by oral gavage for 5 weeks at a dose of 37.5 mg/kg in 90% PEG+10% Chromasolv (Sigma-Aldrich) twice daily, starting on the day of ICN12 injection. When a mouse became terminally sick, it was sacrificed, and the bone marrow and spleen were collected for flow cytometry analysis.

The RCH-ACV human ALL model experiment was conducted by Crown Bioscience (Taicang, China) after approval by the institutional animal care and use committee. During the study, the care and use of animals was conducted in accordance with the regulations of the Association for Assessment and Accreditation of Laboratory Animal Care. We injected  $1 \times 10^6$  RCH-ACV

cells into 20 NOD/SCID mice (10 per group) via tail vein. Ibrutinib treatment (25 mg/kg in 1% methylcellulose, 0.4% Cremephor in water) started the next day; the drug was provided in drinking water. Leukemia expansion was monitored by flow cytometry (human CD19) of whole blood samples. When a mouse became terminally sick, it was sacrificed, and the peripheral blood, bone marrow, and spleen were collected for flow cytometry analysis.

### BLK and BTK knockout using CRISPR-Cas9 system

sgRNA design and cloning were performed according to Ran et al's method<sup>39</sup> with use of a CRISPR design tool (<http://crispr.mit.edu>). Three high-scoring sgRNAs were selected per target. *BLK* and *BTK* targeting sequences were cloned into pSpCas9(BB)-2A-GFP (px458), which was a gift from Dr. Feng Zhang (Addgene plasmid 48138). The px458-based constructs or the empty px458 vector was introduced into RCH-ACV cells by electroporation with the NEON™ Transfection System by using standard protocol 5 (Life Technologies). Viable GFP<sup>+</sup> cells were sorted 72 hours later with FACS Aria Fusion Sorter (BD Biosciences) and used for further experiments. The results obtained with 3 different sgRNAs per target were averaged. Knockout of target genes was verified by western blot analysis of the sorted cells. Additionally, single GFP<sup>+</sup> cells were sorted into 96-well plates to obtain single-cell clones. For sgRNA sequences, the reader is referred to the supplemental Materials and Methods section, available on the *Blood* Web site.

### Data analysis and statistics

Statistical analyses were performed by using Prism 6 for Mac OS X. One sample Student *t* test, unpaired and paired Student *t* tests, Mann-Whitney rank test, Wilcoxon matched-pairs signed-rank test, and log-rank (Mantel-Cox) test were used, as appropriate. *P* values were adjusted for multiple comparisons by using Bonferroni correction. A *P* value of <.05 was considered statistically significant. To reduce variability between individual experiments, we calculated the relative values by dividing the value of a particular sample by the average control value obtained from 0.1% DMSO-treated samples.

For further details on experimental procedures, the reader is referred to the supplemental Materials and Methods section.

## Results

### Pre-BCR-positive ALL is exclusively sensitive to ibrutinib

To explore the functional role of BTK in ALL, we screened a representative panel of ALL cells for BTK expression and activity by western blot (Figure 1A; supplemental Table 1). BTK protein expression was detectable in the majority of ALL cells (17/18) and independent of cytogenetic abnormalities. In contrast, BTK activity (as was indicated by autophosphorylation at residue Y223) was restricted to certain groups of ALL, including BCR-ABL1<sup>+</sup> and pre-BCR<sup>+</sup> cells.

In keeping with an essential role of BTK in the pre-BCR signaling cascade, pBTK<sup>+</sup>/pre-BCR<sup>+</sup> cell lines (RCH-ACV, SMS-SB) were particularly sensitive to BTK-specific tyrosine kinase inhibitor ibrutinib, as was measured by XTT viability/proliferation assay (Figure 1B). Treatment with 0.5 μM of ibrutinib reduced viability/proliferation of RCH-ACV cells by 48.7% (95% confidence interval [CI], 44.6% to 52.9%; *P* < .0001) and of SMS-SB cells by 55.8% (95% CI, 54.2% to 57.5%; *P* < .0001). In contrast, pBTK<sup>+</sup>/pre-BCR<sup>-</sup> lines (TOM-1, NALM-20, NALM-21) and pBTK<sup>-</sup>/pre-BCR<sup>-</sup> lines (REH, RS4;11) were resistant to ibrutinib at concentrations achievable in humans (no significant changes in the presence of 0.5 μM of ibrutinib).<sup>40</sup>

Additional analysis revealed that ibrutinib significantly reduced proliferation of several cell lines (Figure 1C). The reduction was modest

in case of pBTK<sup>+</sup>/pre-BCR<sup>-</sup> cells, with the largest decrease of 14.1% (95% CI, 8.5% to 19.6%; *P* = .0015) observed in NALM-20. In contrast, proliferation of pBTK<sup>+</sup>/pre-BCR<sup>+</sup> RCH-ACV cells was reduced by 39.0% (95% CI, 32.9% to 45.1%; *P* < .0001) and of SMS-SB cells by 42.7% (95% CI, 37.3% to 48.1%; *P* < .0001). Cell viability was not significantly affected by ibrutinib in any cell line, except for RCH-ACV (Figure 1D). However, even in that case the average decrease was quite small (2.1%; 95% CI, 1.3% to 3.0%; *P* = .0007). Taken together, these results suggest that ibrutinib exerts its effects predominantly through the inhibition of cell proliferation rather than through the induction of apoptosis.

### Ibrutinib interferes with induced and tonic pre-BCR signaling

In light of the exclusive sensitivity of pre-BCR<sup>+</sup> ALL cells to ibrutinib, we studied its effects on the activity of the pre-BCR signaling cascade. Pretreatment with ibrutinib completely abrogated pre-BCR-induced calcium flux in pBTK<sup>+</sup>/pre-BCR<sup>+</sup> cells (RCH-ACV, SMS-SB, and Kasumi-2) (Figure 2A-B) and considerably reduced pre-BCR-dependent phosphorylation of Akt and ERK (Figure 2C), thus highlighting the efficacy of ibrutinib in inhibiting ligand-dependent pre-BCR activation.

Along the same lines, ibrutinib abrogated tonic signals from the pre-BCR as indicated by the reduction of Akt phosphorylation in the absence of exogenous pre-BCR stimuli (Figure 2D). Importantly, the degree of pAkt reduction corresponds well with the sensitivity of ALL cells to ibrutinib, thereby suggesting PI3K signaling as one of the main targets of the inhibitor. Consequently, ibrutinib also interfered with phosphorylation of well-established downstream targets of Akt, including tumor suppressive transcription factors FOXO1, FOXO3a, and FOXO4. Reduced phosphorylation of FOXO transcription factors promotes their transcriptional activity, resulting in upregulation of the cell cycle inhibitor p27<sup>Kip</sup> in pre-BCR<sup>+</sup> ALL (Figure 2E-F). Similarly, ibrutinib reduced the phosphorylation of the mTORC1-target ribosomal protein S6, suggesting suppression of mTOR signaling (Figure 2D).

### Ibrutinib induces changes in the pre-BCR signaling pathway and interferes with cell migration

To reveal any long-term effects of ibrutinib on the pre-BCR signaling pathway, we performed gene expression profiling of RCH-ACV cells after 24 and 72 hours' exposure to ibrutinib. QIAGEN's Ingenuity Pathway Analysis indicated B-cell receptor signaling as the most altered pathway after 72 hours (*P* < .0001). Interestingly, prolonged exposure to ibrutinib resulted in suppression of several negative regulators of pre-BCR signaling, such as CD22, CD72, and PTPN6 (SHP-1), at both mRNA and protein levels in pre-BCR<sup>+</sup> cells (Figure 3A-D; supplemental Figure 1). On the other hand, PKCβ, a downstream target of BTK, was upregulated (Figure 3A). Collectively, these changes in gene expression might represent a feedback compensatory mechanism to restore a normal level of pre-BCR signaling activity after inhibition by ibrutinib.

We also observed that ibrutinib significantly downregulated expression of the BCL6 transcription factor, a proposed surrogate marker for pre-BCR activity (Figure 3A-B; supplemental Figure 1).<sup>17</sup> In accordance with previously published data, the drop in BCL6 level coincided with the reduction of CD44 homing receptor expression (Figure 3E).<sup>41</sup> These observations suggest that pre-BCR signaling inhibition with ibrutinib may also interfere with leukemia cells homing to the bone marrow niche.

To further explore the potential of ibrutinib to disrupt the interactions of leukemia cells with their microenvironment, we

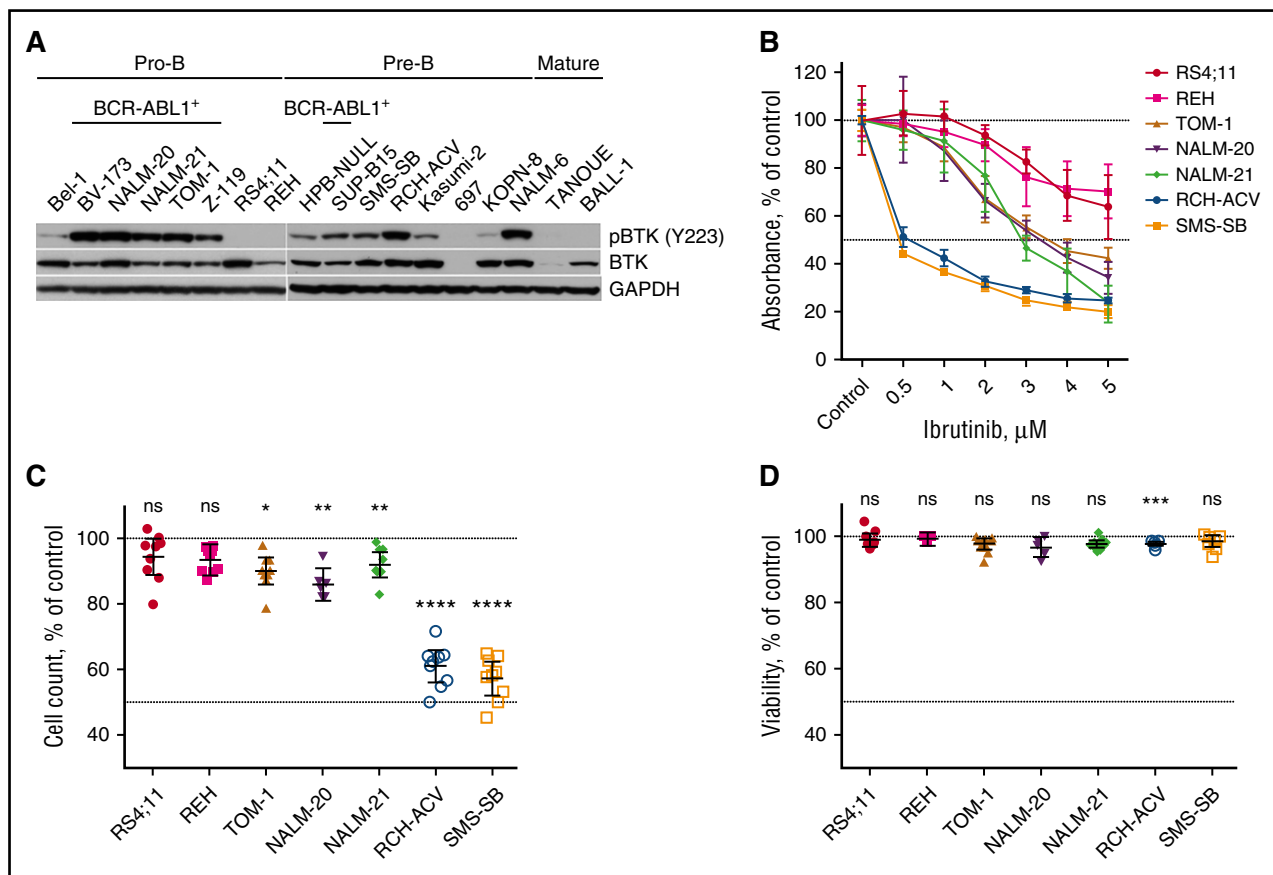


**Figure 1. Several subsets of B-ALL cells have activated BTK, but only pre-BCR<sup>+</sup> ALL cells are sensitive to ibrutinib.** (A) pBTK and total BTK expression in ALL cell lines. (B) Proliferation/viability of different ALL cell lines after ibrutinib treatment as measured by XTT assay. Displayed are the mean with 95% CI from at least 3 independent experiments. (C-D) Comparison of viable cell counts (C) and percentage of viable ALL cells (D) after 96 hours of treatment with 1  $\mu$ M of ibrutinib. Results were normalized to DMSO-treated controls and are presented as the mean with 95% CI from 3 independent experiments. ns, not significant. \* $P < .05$ ; \*\* $P < .01$ ; \*\*\* $P < .001$ ; \*\*\*\* $P < .0001$ .

measured ALL cell chemotaxis toward CXCL12 after treatment with the inhibitor. Interestingly, ibrutinib significantly inhibited the migration of pre-BCR<sup>-</sup> REH cells and pre-BCR<sup>+</sup> RCH-ACV cells (Figure 3F). Pretreatment with ibrutinib reduced the REH cell chemotaxis toward CXCL12 from 71.8% (95% CI, 65.7% to 77.9%) to 46.5% (95% CI, 37.7% to 55.4%;  $P = .01$ ), and the migration of RCH-ACV dropped from 10.5% (95% CI, 3.1% to 17.7%) to 6.5% (95% CI, 1.0% to 11.9%;  $P = .0152$ ). Ibrutinib-treated RCH-ACV cells migrated beneath KUSA-H1 bone marrow stromal cells (BMSC) significantly less effectively than did control cells (4.8%; 95% CI, 3.5% to 6.0% vs. 11.5%; 95% CI, 7.9% to 15.1%;  $P = .0022$ ) (Figure 3G; supplemental Figure 2). The reduction in the REH cell migration was smaller. Taken together, these results indicate that ibrutinib interferes in multiple ways with leukemia cell interactions with their supportive microenvironment.

#### Ibrutinib acts through multiple targets in ALL

To further elucidate the mechanism of action of ibrutinib in pre-BCR<sup>+</sup> ALL, we selectively knocked out the *BTK* gene (*BTK* KO) in RCH-ACV cells using CRISPR-Cas9 gene editing and subsequently measured their proliferation rate by XTT assay. Surprisingly, despite their sensitivity to ibrutinib, RCH-ACV cells were quite resistant to the loss of BTK protein expression: the maximum observed decrease in proliferation was only 15.7% (95% CI, 9.6% to 21.8%;  $P = .0143$ ) (Figure 4A; supplemental Figure 3). Furthermore, treatment with 0.5  $\mu$ M of ibrutinib reduced proliferation of both *BTK* KO and *BTK*

wild-type cells to about 43% of that of the control untreated cells, indicating the importance of alternative targets for the activity of ibrutinib in pre-BCR<sup>+</sup> ALL.

Ibrutinib has been previously reported to target tyrosine kinases other than BTK.<sup>42-44</sup> According to in vitro kinase assays, ibrutinib irreversibly inhibits 8 kinases with IC<sub>50</sub> below 1  $\mu$ M.<sup>42</sup> In our search for additional targets of ibrutinib, we therefore analyzed the expression of these kinases in a subset of pre-BCR<sup>+</sup> ALL using publicly available microarray data from the St. Jude Children's Hospital.<sup>37</sup> Among those, only *BTK* and *BLK* were significantly overexpressed in pre-BCR<sup>+</sup> ALL in comparison with other subtypes (Figure 4B). Importantly, *BLK* is a part of the BCR and pre-BCR signaling cascades, functioning upstream of BTK.<sup>45,46</sup> Thus, we hypothesized that *BLK* might serve as an additional target of ibrutinib in pre-BCR<sup>+</sup> ALL.

To study the role of *BLK* for the effects of ibrutinib, we generated RCH-ACV cells lacking *BLK* (*BLK* KO) or both *BLK* and *BTK* (*BLK/BTK* KO). The proliferation rate of RCH-ACV cells seemed to be more sensitive to *BLK* KO (reduction by 20.7% in comparison with untreated cells transfected with the empty vector; 95% CI, 18.7% to 22.6%;  $P < .0001$ ) than to *BTK* KO (reduction by 14.2%; 95% CI, 9.8% to 18.5%;  $P = .0003$ ), and even more so to double *BLK/BTK* KO (reduction by 33.8%; 95% CI, 27.1% to 40.5%;  $P < .0001$ ) (Figure 4C). Although ibrutinib could still significantly suppress proliferation of all types of cells, its effect was smaller in knockout cells: proliferation of control cells was reduced by 54.5% (95% CI, 51.3% to 57.7%;  $P < .0001$ ), of *BTK* KO by 43.1% (95% CI, 40.2% to 46.1%;  $P < .0001$ ), of *BLK* KO by 33.3% (95% CI, 31.6% to 34.9%;  $P < .0001$ ),

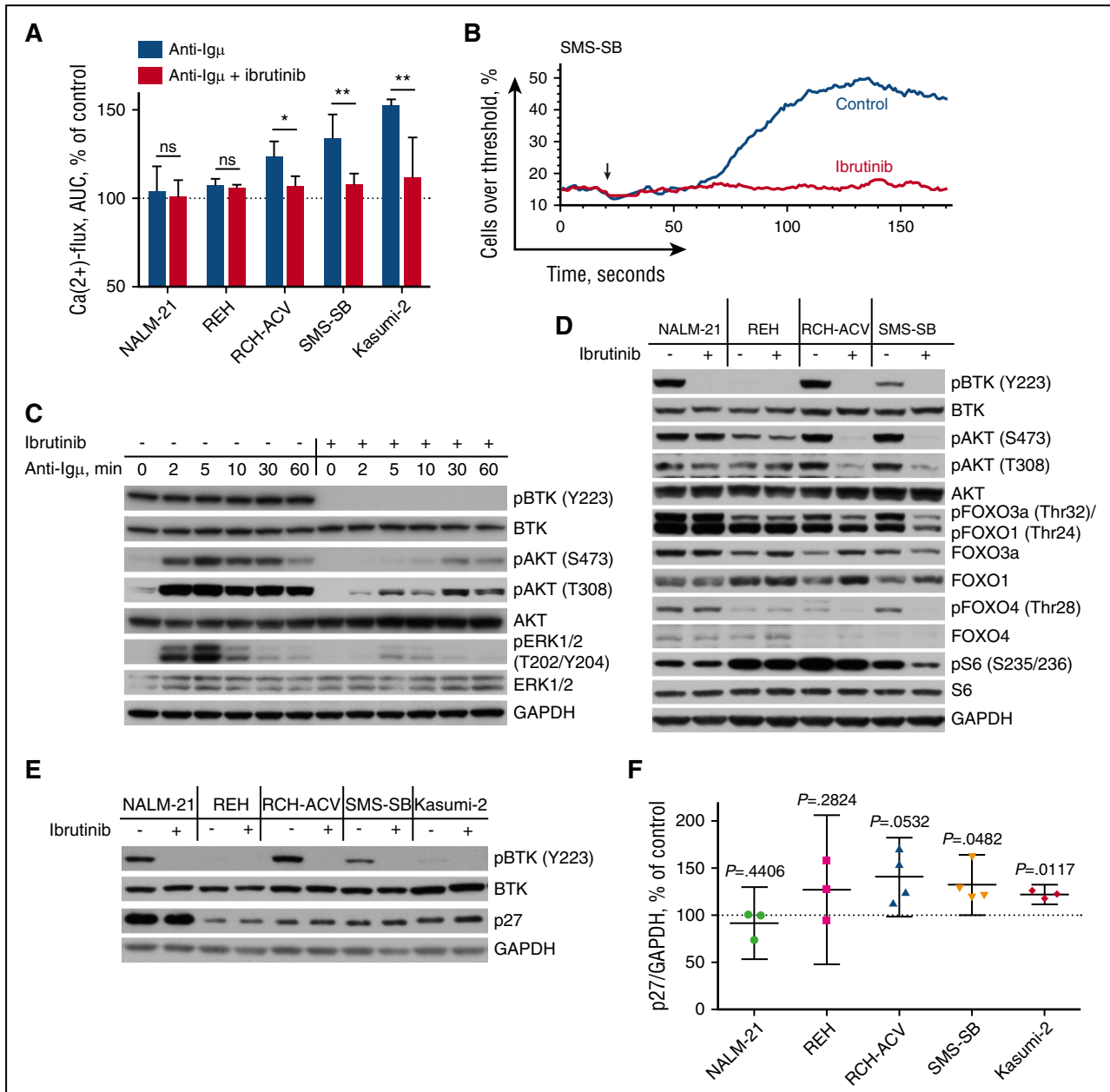


**Figure 2. Ibrutinib thwarts pre-BCR signaling in B-ALL.** (A) Ca<sup>2+</sup> mobilization in B-ALL cells after pre-BCR cross-linking with anti-Ig $\mu$ . ALL cells were pretreated with 1  $\mu$ M of ibrutinib or without. The background fluorescence threshold was established at the fluorescence intensity of 85th percentile of unstimulated cells. Area under the curve was calculated and normalized to a background reading of a particular sample and then to the response of control cells. Displayed are the means with 95% CI from 3–6 independent experiments. (B) Representative display of Ca<sup>2+</sup> mobilization in pre-BCR<sup>+</sup> B-ALL cells after anti-Ig $\mu$  stimulation (indicated by the arrow), with or without ibrutinib pretreatment. (C) Western blot showing that ibrutinib treatment effectively abrogates anti-Ig $\mu$ -induced pre-BCR-dependent BTK, Akt, and ERK activation in RCH-ACV cells. (D) Western blot showing that treatment with 0.5  $\mu$ M of ibrutinib for 1 hour suppresses baseline Akt signaling in pre-BCR<sup>+</sup> (RCH-ACV, SMS-SB) but not in pre-BCR<sup>-</sup> (NALM-21, REH) B-ALL. (E–F) Western blot analysis of p27 content in ALL cells exposed to ibrutinib for 24 hours (E) and densitometry of 3–4 independent experiments presented as the mean with 95% CI (F). AUC, area under the curve. ns, not significant. \**P* < .05; \*\**P* < .01.

and of *BLK/BTK* KO by 25.4% (95% CI, 20.6% to 30.3%; *P* < .0001). Consistently, only double *BTK/BLK* KO reduced Akt and ERK phosphorylation in RCH-ACV to levels comparable to cells treated with ibrutinib (Figure 4D). Nonetheless, the effect of double knockout was not quite equal to that of ibrutinib, suggesting that other covalent or noncovalent targets are involved in the mechanism of its action.

To quantitatively measure how the absence of ibrutinib targets affects the sensitivity of ALL cells to the drug, we generated several RCH-ACV-derived clones, lacking BTK, BLK, or both. The average IC<sub>50</sub> of ibrutinib in control clones was considerably lower (455 nM;

95% CI, 372–556 nM; *N* = 5) than in *BLK* KO (938 nM; 95% CI, 775–1136 nM; *N* = 6), *BTK* KO (1305 nM; 95% CI, 1099–1551 nM; *N* = 4), or double *BLK/BTK* KO clones (1698 nM; 95% CI, 1400–2060 nM; *N* = 4) (Figure 4E). These results further confirm our hypothesis that ibrutinib requires both BTK and BLK for its maximum efficacy in ALL.

#### Ibrutinib induces apoptosis of primary ALL cells

To further evaluate ibrutinib as a potential therapeutic agent in ALL, we treated peripheral blood mononuclear cells from 7 patients with ALL with increasing concentrations of the inhibitor (supplemental Table 2

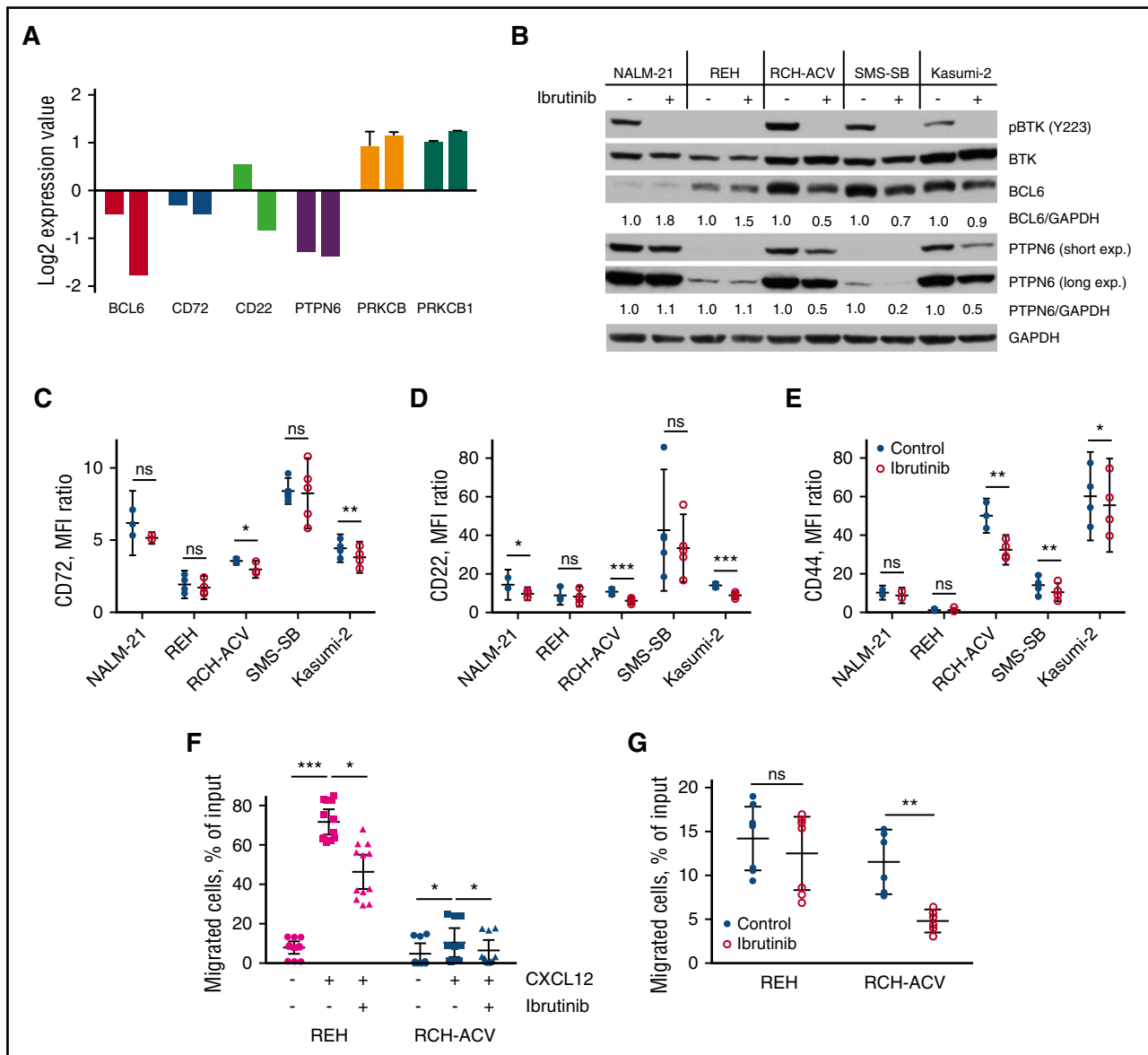


**Figure 3. Ibrutinib affects pre-BCR signaling pathway components and cell migration.** (A) Results of gene expression profiling for selected genes of pre-BCR<sup>+</sup> B-ALL cells (RCH-ACV) treated with ibrutinib for 24 hours (left bar in each pair) or 72 hours (right bar in each pair). Values were normalized to controls (DMSO-treated cells); data from multiple probes were averaged when available; displayed are the mean  $\pm$  SD. (B) PTPN6 and BCL6 protein levels were reduced in pre-BCR<sup>+</sup> (RCH-ACV, SMS-SB, Kasumi-2), but not in pre-BCR<sup>-</sup> (NALM-21, REH), B-ALL cells after treatment with 0.5  $\mu$ M of ibrutinib for 72 hours. BCL6 and PTPN6 signals were quantified by densitometry and normalized to corresponding GAPDH measurements and subsequently to untreated controls. Short and long exp., short and long exposition. (C-E) CD72, CD22, and CD44 surface expression after 72 hours of ibrutinib treatment as measured by flow cytometry. Results of 3–5 independent experiments presented as the mean fluorescence intensity ratio, mean with 95% CI. (F) Pretreatment with ibrutinib inhibited migration of ALL cells toward CXCL12 in chamber chemotaxis assay. Numbers of transmigrated cells were measured in triplicate in 3–4 independent experiments, were normalized to 1:20 dilution of input cells, and are presented as the mean with 95% CI. (G) Treatment with ibrutinib for 72 hours significantly decreased spontaneous migration of RCH-ACV cells beneath KUSA-H1 stromal cells. Results of 2 independent experiments are displayed as the mean with 95% CI. MFI, mean fluorescence intensity. ns, not significant. \* $P < .05$ ; \*\* $P < .01$ ; \*\*\* $P < .001$ .

summarizes patients' characteristics). Ibrutinib induced mild but significant levels of apoptosis of leukemic cells: 0.5  $\mu$ M of ibrutinib reduced viability by 5.5% (95% CI, 0.4% to 10.7%;  $P = .0313$ ), and 1  $\mu$ M of ibrutinib reduced viability by 12.3% (95% CI, 2.9% to 21.7%;  $P = .0156$ ) (Figure 5A-B). These results are in agreement with similar data on chronic lymphocytic leukemia (CLL) cells cultured ex vivo, for which ibrutinib also demonstrates only a moderate effect on viability.<sup>27,28</sup> Relative sensitivity to ibrutinib of the sample ALL 4 (19.2% reduction in viability by 1  $\mu$ M of ibrutinib) correlated with a more pronounced decrease in the levels of phosphorylated Akt and S6 proteins when compared with less sensitive sample ALL 6 (0.2% reduction in viability) (Figure 5C).

#### Ibrutinib treatment significantly prolongs survival in ALL mouse models

Finally, we sought to examine in vivo efficacy of ibrutinib against pre-BCR<sup>+</sup> ALL. The RCH-ACV cell line and xenograft-amplified primary sample ICN12<sup>17</sup> were chosen for this purpose. ICN12 cells were sensitive to ibrutinib under in vitro conditions with IC<sub>50</sub> of 2.6  $\mu$ M (95% CI, 2.4–2.9  $\mu$ M) (data not shown) and demonstrated a characteristic response to ibrutinib treatment, such as reduction in pAkt, pERK, BCL6, and PTPN6 (supplemental Figure 4). These cells were injected into NOD/SCID mice, and animals were treated with 37.5 mg/kg ibrutinib twice daily through oral gavage for 5 weeks, starting at the day

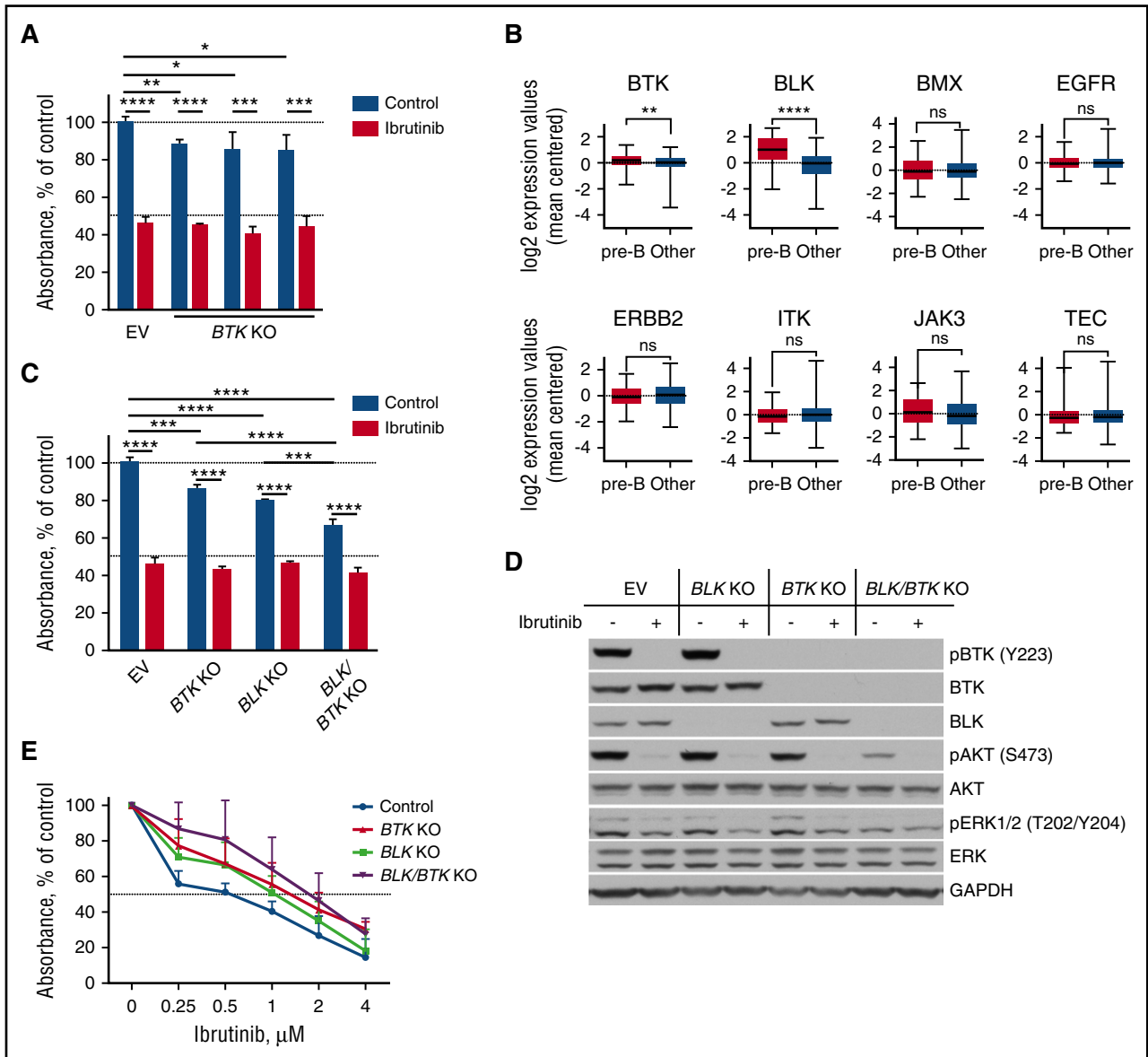


**Figure 4. Ibrutinib targets BTK and BLK in B-ALL.** (A) Proliferation of RCH-ACV cells after *BTK* gene knockout was reduced, when quantified in XTT assays and compared with empty vector (EV) controls. Three different sgRNAs were used to knockout *BTK*. Displayed are the mean with 95% CI of triplicates. (B) The box and whisker graphs depict relative gene expression of tyrosine kinases, to which ibrutinib binds covalently, in primary ALL cases from the St. Jude Children’s Hospital dataset. The whiskers represent minimum and maximum expression values. *BTK* and *BLK* expression levels were significantly higher in pre-BCR<sup>+</sup> ALL subset than in all other subsets. (C) *BTK*, *BLK*, and especially double *BLK/BTK* gene knockout considerably reduced proliferation of RCH-ACV as measured by XTT assay. Displayed are the mean with 95% CI of triplicates. (D) Double *BLK/BTK* KO RCH-ACV cells demonstrated diminished phosphorylation of Akt and ERK similarly to control (empty vector) cells treated with 0.5  $\mu$ M of ibrutinib for 1 hour. (E) Individual *BTK* and *BLK* KO RCH-ACV cells were expanded to generate clones. The dose-response curves demonstrate lower ibrutinib sensitivity of KO clones in comparison with empty vector controls as measured by XTT assay. Depicted are the mean with 95% CI of 4–6 clones of each type. ns, not significant. \* $P < .05$ ; \*\* $P < .01$ ; \*\*\* $P < .001$ ; \*\*\*\* $P < .0001$ .

of injection. The mice receiving treatment survived significantly longer than did untreated animals: the median survival time (MST) with treatment was 70 days in comparison with 52 days in the control group (Figure 6A-B).

Survival time in the RCH-ACV ALL model was much shorter, indicating a more aggressive disease. Nevertheless, ibrutinib treatment significantly prolonged survival of mice, with MST of 23 days in controls versus 25 days in the treatment group (Figure 6C).

Favorable combination partners could further enhance considerable efficacy that ibrutinib demonstrated as a single agent in mouse models of human ALL. Combinations of ibrutinib with dexamethasone or vincristine synergistically reduced viability and proliferation of

pre-BCR<sup>+</sup> ALL cells, as was demonstrated by combination indices of less than 1 (Figure 6D).

Taken together, the data from our in vitro and in vivo experiments indicate that ibrutinib has therapeutic activity against human pre-BCR<sup>+</sup> ALL cells, as a single agent and more potently in combination with conventional chemotherapy.

## Discussion

The goal of this study was to evaluate effects of ibrutinib on ALL cell proliferation and survival and the importance of BTK and BLK

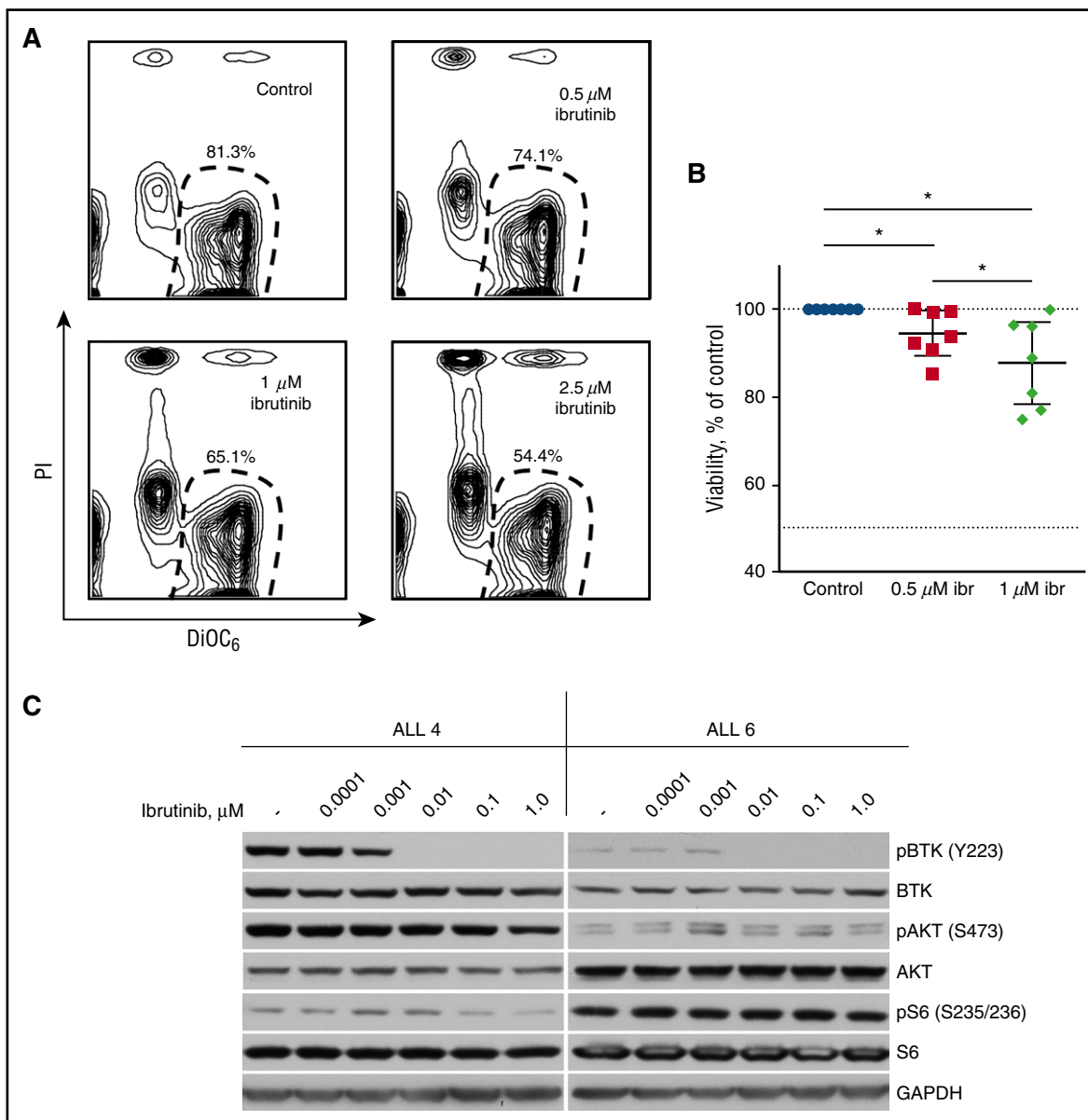


**Figure 5. Ibrutinib induces apoptosis of primary ALL cells.** (A) Primary ALL cells cocultured with KUSA-H1 stromal cells were treated with ibrutinib (ibr) for 48 hours. Representative counter plots show a fraction of viable ALL cells as determined by DiOC<sub>6</sub>/PI staining and flow cytometry. (B) Ibrutinib significantly reduced viability of primary ALL cells after 48 hours of treatment. Percentage of viable ALL cells was normalized to DMSO-treated control. Displayed are the mean with 95% CI of 7 ALL samples. (C) Ibrutinib inhibits Akt in sensitive ALL cells (ALL 4) but not in insensitive cells (ALL 6), as determined by western blotting. \**P* < .05.

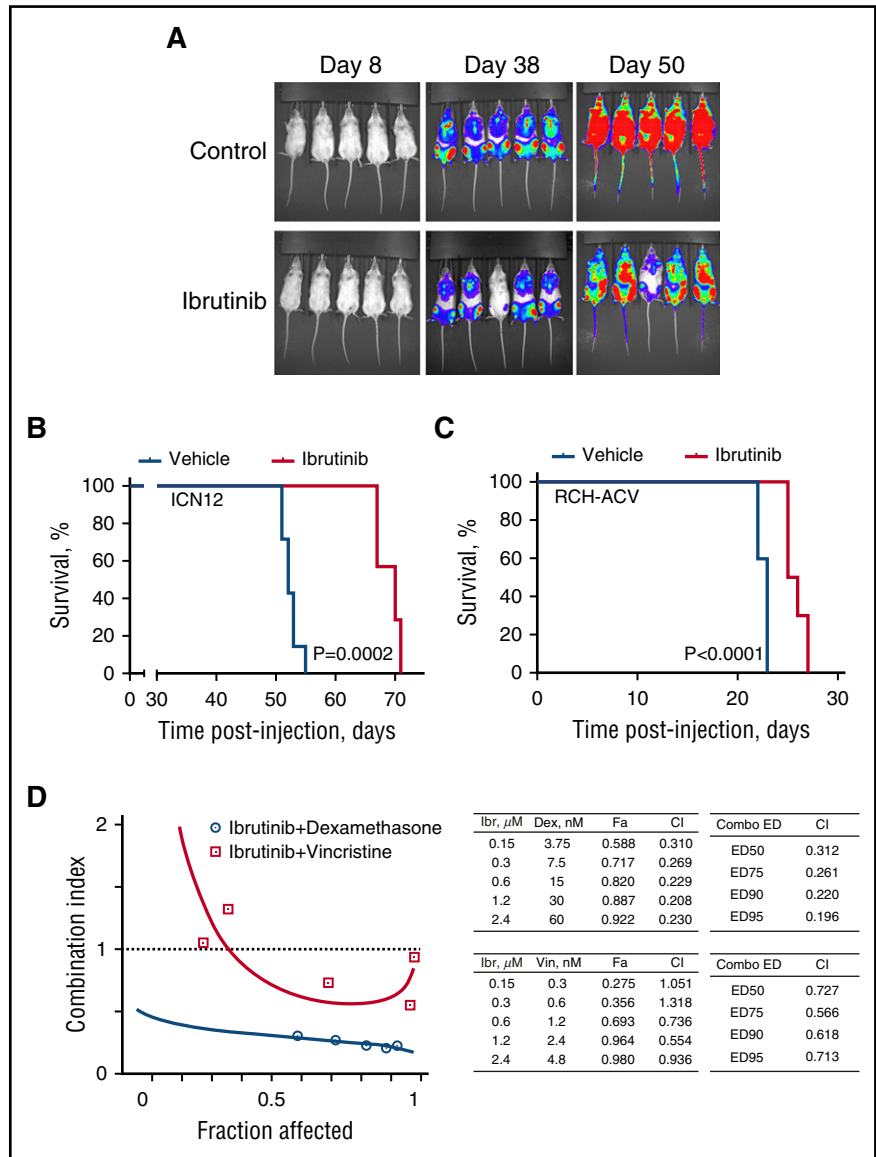
inhibition. BTK is the principal known target of ibrutinib, and we found activated BTK in BCR-ABL1<sup>+</sup> and pre-BCR<sup>+</sup> cells; however, only pre-BCR<sup>+</sup> ALL cells were sensitive to ibrutinib at clinically relevant concentrations. In such pre-BCR<sup>+</sup> ALL cells, ibrutinib abrogated induced and autonomous pre-BCR signaling, resulting in deactivation of Akt and its downstream targets, and thwarted ALL cells' proliferation. Ibrutinib treatment caused several long-term effects on pre-BCR signaling and related signaling pathways, on the basis of our gene expression studies. Expression of positive and negative regulators of pre-BCR signaling was altered, presumably via compensatory mechanisms activated by continuous blockade of BTK activity. Similar compensatory changes were reported in t(1;19)-ALL cells after pre-BCR signaling suppression with dasatinib.<sup>19,47</sup> Interestingly, after initial reduction by dasatinib, the level of phosphorylated Akt recovered because of increased ROR1/MEK/ERK signaling.

Ibrutinib treatment also resulted in substantial reduction of BCL6, which plays a role in limiting pre-B-cell proliferation and in induction of quiescence.<sup>48</sup> BCL6 is constitutively expressed in pre-BCR<sup>+</sup> ALL due to tonic pre-BCR signaling, and its knockdown or inhibition decelerates proliferation of these cells.<sup>17</sup> Possibly the amount of BCL6 in cells determines their fate; lower BCL6 levels promote quiescence, and higher levels support their malignant growth.<sup>49</sup> Following this rationale, one may argue that suppression of BCL6 by ibrutinib may contribute to deceleration of ALL cell growth.

Similar to its effects in other hematologic malignancies, ibrutinib affected the complex interactions of ALL cells with their microenvironment.<sup>28,50-56</sup> It inhibited the migration of both pre-BCR<sup>+</sup> and pre-BCR<sup>-</sup> ALL cells toward CXCL12 and beneath BMSC, which is similar to what has been demonstrated in mature B-cell leukemia



**Figure 6. Ibrutinib prolongs survival in xenograft models of human ALL.** (A) Engraftment and expansion of ICN12-induced leukemia in mice treated with ibrutinib or vehicle control as visualized by luciferase bioimaging. (B) Kaplan-Meier curve demonstrates significantly longer overall survival of ibrutinib-treated mice in a ICN12 human ALL model when compared with control mice (7 per group). (C) Kaplan-Meier curve demonstrates significantly longer overall survival of ibrutinib-treated mice in a RCH-ACV human ALL model when compared with control mice (10 per group). (D) Cotreatment with ibrutinib and the chemotherapy agents dexamethasone or vincristine synergistically reduced the amount of metabolically active RCH-ACV cells when measured in XTT assays (Fa-CI plot). Combination indices (CI) were calculated on the basis of triplicate measurements using CompuSyn. Left-hand side tables include CIs for the actual experimental points. Right-hand side tables contain CIs for various effective doses of the drug combination, as is indicated. ED, effective dose; Ibr, ibrutinib; Dex, dexamethasone; Vin, vincristine.



(CLL)<sup>28,55</sup> and proposed as a mechanism involved in redistribution of leukemia cells from tissues into the blood.<sup>40,57</sup>

Using CRISPR-Cas9-mediated genome editing, we demonstrated that *BTK* KO could not fully recapitulate the effects of ibrutinib on pre-BCR<sup>+</sup> RCH-ACV cells. We searched for additional targets of the drug and identified *BLK*. Along with *LYN* and *FYN*, *BLK* is one of the several *Src* family tyrosine kinases in B cells that can transfer signals from the activated pre-BCR to *SYK*.<sup>45,58</sup> Interestingly, upregulated *BLK* expression was recently identified as part of a 40-gene signature of pre-BCR<sup>+</sup> versus pre-BCR<sup>-</sup> ALL.<sup>17</sup> We found that double *BLK/BTK* KO resembles effects of ibrutinib treatment more than *BLK* or *BTK* KO alone, suggesting that both targets are of importance in ALL. These findings agree with a previous report that knockdown of either *BLK* or *BTK* alone does not considerably affect viability and proliferation of pre-BCR<sup>+</sup> ALL cells.<sup>19</sup>

In summary, we demonstrate that ibrutinib suppresses proliferation of pre-BCR<sup>+</sup> ALL, in vitro and in vivo, by targeting two components of pre-BCR signaling pathway: *BTK* and *BLK*. Ibrutinib showed great efficacy and significantly prolonged survival in mouse xenograft

models of pre-BCR<sup>+</sup> ALL. These results indicate that the anti-proliferative effect of ibrutinib observed in ALL cells in vitro translates into a similar effect in vivo and provides a rationale for exploring the clinical activity of ibrutinib in patients with pre-BCR<sup>+</sup> ALL.

### Acknowledgments

The work was supported by a Leukemia & Lymphoma Society Scholar Award in Clinical Research (J.A.B.), and by Janssen Research & Development. This research is also supported in part by the Anderson Cancer Center Support Grant CA016672. STR DNA fingerprinting was done by the Cancer Center Support Grant-funded Characterized Cell Line core, National Institutes of Health National Cancer Institute CA016672. Cell sorting was performed in the Flow Cytometry & Cellular Imaging Facility, which is supported in part by the National Institutes of Health through Anderson Cancer Center Support Grant CA016672.

## Authorship

Contribution: E.K. performed the experiments, analyzed the data, prepared the figures and wrote the manuscript; C.H. performed the mouse model experiments and prepared the figures; S.K. participated in planning and performing some of the experiments and wrote the manuscript; Z.W. generated the gene expression profiling data; S.B. discussed the results, designed and arranged the mouse model experiments, and reviewed the manuscript; B.Y.C. provided a vital reagent and reviewed the manuscript; M.M. provided the PDX cell lines and reviewed the manuscript; R.E.D.

analyzed the gene expression profile data and reviewed the manuscript; J.A.B. designed the research, supervised the study, and wrote the manuscript. All authors approved the final version of the manuscript to be published.

Conflict-of interest-disclosure: J.A.B. received research funding from Pharmacyclics, Inc. S.B. is an employee of Janssen Research & Development. B.Y.C. is an employee of Pharmacyclics, an AbbVie company, and holds stocks from AbbVie.

Correspondence: Jan A. Burger, Department of Leukemia, University of Texas MD Anderson Cancer Center, Unit 428, PO Box 301402, Houston, TX 77230-1402; e-mail: jaburger@mdanderson.org.

## References

- Zhou Y, You MJ, Young KH, et al. Advances in the molecular pathobiology of B-lymphoblastic leukemia. *Hum Pathol*. 2012;43(9):1347-1362.
- Inaba H, Greaves M, Mullighan CG. Acute lymphoblastic leukaemia. *Lancet*. 2013; 381(9881):1943-1955.
- Daver N, O'Brien S. Novel therapeutic strategies in adult acute lymphoblastic leukemia—a focus on emerging monoclonal antibodies. *Curr Hematol Malig Rep*. 2013;8(2):123-131.
- Young RM, Staudt LM. Targeting pathological B cell receptor signalling in lymphoid malignancies. *Nat Rev Drug Discov*. 2013;12(3): 229-243.
- Burger JA. Bruton's tyrosine kinase (BTK) inhibitors in clinical trials. *Curr Hematol Malig Rep*. 2014;9(1):44-49.
- Herzog S, Reth M, Jumaa H. Regulation of B-cell proliferation and differentiation by pre-B-cell receptor signalling. *Nat Rev Immunol*. 2009;9(3): 195-205.
- Hendriks RW, Kersseboom R. Involvement of SLP-65 and Btk in tumor suppression and malignant transformation of pre-B cells. *Semin Immunol*. 2006;18(1):67-76.
- Rolink AG, Winkler T, Melchers F, Andersson J. Precursor B cell receptor-dependent B cell proliferation and differentiation does not require the bone marrow or fetal liver environment. *J Exp Med*. 2000;191(1):23-32.
- Ohnishi K, Melchers F. The nonimmunoglobulin portion of lambda5 mediates cell-autonomous pre-B cell receptor signaling. *Nat Immunol*. 2003; 4(9):849-856.
- Köhler F, Hug E, Eschbach C, et al. Autoreactive B cell receptors mimic autonomous pre-B cell receptor signaling and induce proliferation of early B cells. *Immunity*. 2008;29(6):912-921.
- Gauthier L, Rossi B, Roux F, Termine E, Schiff C. Galectin-1 is a stromal cell ligand of the pre-B cell receptor (BCR) implicated in synapse formation between pre-B and stromal cells and in pre-BCR triggering. *Proc Natl Acad Sci USA*. 2002;99(20): 13014-13019.
- Klein F, Feldhahn N, Harder L, et al. The BCR-ABL1 kinase bypasses selection for the expression of a pre-B cell receptor in pre-B acute lymphoblastic leukemia cells. *J Exp Med*. 2004; 199(5):673-685.
- Klein F, Feldhahn N, Herzog S, et al. BCR-ABL1 induces aberrant splicing of IKAROS and lineage infidelity in pre-B lymphoblastic leukemia cells. *Oncogene*. 2006;25(7):1118-1124.
- Feldhahn N, Río P, Soh BN, et al. Deficiency of Bruton's tyrosine kinase in B cell precursor leukemia cells. *Proc Natl Acad Sci USA*. 2005; 102(37):13266-13271.
- Mullighan CG, Miller CB, Radtke I, et al. BCR-ABL1 lymphoblastic leukaemia is characterized by the deletion of Ikaros. *Nature*. 2008;453(7191): 110-114.
- Trageser D, Iacobucci I, Nahar R, et al. Pre-B cell receptor-mediated cell cycle arrest in Philadelphia chromosome-positive acute lymphoblastic leukemia requires IKAROS function. *J Exp Med*. 2009;206(8):1739-1753.
- Geng H, Hurtz C, Lenz KB, et al. Self-enforcing feedback activation between BCL6 and pre-B cell receptor signaling defines a distinct subtype of acute lymphoblastic leukemia. *Cancer Cell*. 2015; 27(3):409-425.
- Hunger SP. Chromosomal translocations involving the E2A gene in acute lymphoblastic leukemia: clinical features and molecular pathogenesis. *Blood*. 1996;87(4):1211-1224.
- Biococca VT, Chang BH, Masouleh BK, et al. Crosstalk between ROR1 and the Pre-B cell receptor promotes survival of t(1;19) acute lymphoblastic leukemia. *Cancer Cell*. 2012;22(5): 656-667.
- Köhler S, Havranek O, Seyfried F, et al. Pre-BCR signaling in precursor B-cell acute lymphoblastic leukemia regulates PI3K/AKT, FOXO1 and MYC, and can be targeted by SYK inhibition. *Leukemia*. 2016;30(6):1246-1254.
- Geneviev HC, Hinshelwood S, Gaspar HB, et al. Expression of Bruton's tyrosine kinase protein within the B cell lineage. *Eur J Immunol*. 1994; 24(12):3100-3105.
- Nisitani S, Satterthwaite AB, Akashi K, Weissman IL, Witte ON, Wahl MI. Posttranscriptional regulation of Bruton's tyrosine kinase expression in antigen receptor-stimulated splenic B cells. *Proc Natl Acad Sci USA*. 2000;97(6):2737-2742.
- Smith CI, Baskin B, Humire-Greif P, et al. Expression of Bruton's agammaglobulinemia tyrosine kinase gene, BTK, is selectively down-regulated in T lymphocytes and plasma cells. *J Immunol*. 1994;152(2):557-565.
- Mohamed AJ, Yu L, Bäckesjö CM, et al. Bruton's tyrosine kinase (Btk): function, regulation, and transformation with special emphasis on the PH domain. *Immunol Rev*. 2009;228(1):58-73.
- Buggy JJ, Elias L. Bruton tyrosine kinase (BTK) and its role in B-cell malignancy. *Int Rev Immunol*. 2012;31(2):119-132.
- Satterthwaite AB, Witte ON. The role of Bruton's tyrosine kinase in B-cell development and function: a genetic perspective. *Immunol Rev*. 2000;175:120-127.
- Herman SE, Gordon AL, Hertlein E, et al. Bruton tyrosine kinase represents a promising therapeutic target for treatment of chronic lymphocytic leukemia and is effectively targeted by PCI-32765. *Blood*. 2011;117(23):6287-6296.
- Ponader S, Chen SS, Buggy JJ, et al. The Bruton tyrosine kinase inhibitor PCI-32765 thwarts chronic lymphocytic leukemia cell survival and tissue homing in vitro and in vivo. *Blood*. 2012;119(5):1182-1189.
- Davis RE, Ngo VN, Lenz G, et al. Chronic active B-cell-receptor signalling in diffuse large B-cell lymphoma. *Nature*. 2010;463(7277):88-92.
- Katz FE, Lovering RC, Bradley LA, et al. Expression of the X-linked agammaglobulinemia gene, btk in B-cell acute lymphoblastic leukemia. *Leukemia*. 1994;8(4):574-577.
- Goodman PA, Wood CM, Vassilev AO, Mao C, Uckun FM. Defective expression of Bruton's tyrosine kinase in acute lymphoblastic leukemia. *Leuk Lymphoma*. 2003;44(6):1011-1018.
- Feldhahn N, Klein F, Mooster JL, et al. Mimicry of a constitutively active pre-B cell receptor in acute lymphoblastic leukemia cells. *J Exp Med*. 2005; 201(11):1837-1852.
- van der Veer A, van der Velden VH, Willemse ME, et al. Interference with pre-B-cell receptor signaling offers a therapeutic option for TCF3-rearranged childhood acute lymphoblastic leukemia. *Blood Cancer J*. 2014;4:e181.
- Burger JA, Tsukada N, Burger M, Zvaifler NJ, Dell'Aquila M, Kippis TJ. Blood-derived nurse-like cells protect chronic lymphocytic leukemia B cells from spontaneous apoptosis through stromal cell-derived factor-1. *Blood*. 2000;96(8):2655-2663.
- Quiroga MP, Balakrishnan K, Kurtova AV, et al. B-cell antigen receptor signaling enhances chronic lymphocytic leukemia cell migration and survival: specific targeting with a novel spleen tyrosine kinase inhibitor, R406. *Blood*. 2009; 114(5):1029-1037.
- Ma W, Wang M, Wang ZQ, et al. Effect of long-term storage in TRIzol on microarray-based gene expression profiling. *Cancer Epidemiol Biomarkers Prev*. 2010;19(10):2445-2452.
- Zhang J, Ding L, Holmfeldt L, et al. The genetic basis of early T-cell precursor acute lymphoblastic leukaemia. *Nature*. 2012;481(7380):157-163.
- Burger JA, Burger M, Kippis TJ. Chronic lymphocytic leukemia B cells express functional CXCR4 chemokine receptors that mediate spontaneous migration beneath bone marrow stromal cells. *Blood*. 1999;94(11):3658-3667.
- Ran FA, Hsu PD, Wright J, Agarwala V, Scott DA, Zhang F. Genome engineering using the CRISPR-Cas9 system. *Nat Protoc*. 2013;8(11): 2281-2308.
- Advani RH, Buggy JJ, Sharman JP, et al. Bruton tyrosine kinase inhibitor ibrutinib (PCI-32765) has significant activity in patients with relapsed/refractory B-cell malignancies. *J Clin Oncol*. 2013;31(1):88-94.
- Duy C, Hurtz C, Shojaaee S, et al. BCL6 enables Ph+ acute lymphoblastic leukaemia cells to survive BCR-ABL1 kinase inhibition. *Nature*. 2011;473(7347):384-388.

42. Honigberg LA, Smith AM, Sirisawad M, et al. The Bruton tyrosine kinase inhibitor PCI-32765 blocks B-cell activation and is efficacious in models of autoimmune disease and B-cell malignancy. *Proc Natl Acad Sci USA*. 2010;107(29):13075-13080.
43. Dubovsky JA, Beckwith KA, Natarajan G, et al. Ibrutinib is an irreversible molecular inhibitor of ITK driving a Th1-selective pressure in T lymphocytes. *Blood*. 2013;122(15):2539-2549.
44. Lanning BR, Whitby LR, Dix MM, et al. A road map to evaluate the proteome-wide selectivity of covalent kinase inhibitors. *Nat Chem Biol*. 2014;10(9):760-767.
45. Aoki Y, Isselbacher KJ, Cherayil BJ, Pillai S. Tyrosine phosphorylation of Blk and Fyn Src homology 2 domain-binding proteins occurs in response to antigen-receptor ligation in B cells and constitutively in pre-B cells. *Proc Natl Acad Sci USA*. 1994;91(10):4204-4208.
46. Burkhardt AL, Brunswick M, Bolen JB, Mond JJ. Anti-immunoglobulin stimulation of B lymphocytes activates src-related protein-tyrosine kinases. *Proc Natl Acad Sci USA*. 1991;88(16):7410-7414.
47. Hantschel O, Rix U, Schmidt U, et al. The Btk tyrosine kinase is a major target of the Bcr-Abl inhibitor dasatinib. *Proc Natl Acad Sci USA*. 2007;104(33):13283-13288.
48. Nahar R, Ramezani-Rad P, Mossner M, et al. Pre-B cell receptor-mediated activation of BCL6 induces pre-B cell quiescence through transcriptional repression of MYC. *Blood*. 2011;118(15):4174-4178.
49. Rickert RC. New insights into pre-BCR and BCR signalling with relevance to B cell malignancies. *Nat Rev Immunol*. 2013;13(8):578-591.
50. Zaitseva L, Murray MY, Shafat MS, et al. Ibrutinib inhibits SDF1/CXCR4 mediated migration in AML. *Oncotarget*. 2014;5(20):9930-9938.
51. Pillinger G, Abdul-Aziz A, Zaitseva L, et al. Targeting BTK for the treatment of FLT3-ITD mutated acute myeloid leukemia. *Sci Rep*. 2015;5:12949.
52. Rushworth SA, Pillinger G, Abdul-Aziz A, et al. Activity of Bruton's tyrosine-kinase inhibitor ibrutinib in patients with CD117-positive acute myeloid leukaemia: a mechanistic study using patient-derived blast cells. *Lancet Haematol*. 2015;2(5):e204-e211.
53. Bernard S, Danglade D, Gardano L, et al. Inhibitors of BCR signalling interrupt the survival signal mediated by the micro-environment in mantle cell lymphoma. *Int J Cancer*. 2015;136(12):2761-2774.
54. Sivina M, Kreitman RJ, Arons E, Ravandi F, Burger JA. The bruton tyrosine kinase inhibitor ibrutinib (PCI-32765) blocks hairy cell leukaemia survival, proliferation and B cell receptor signalling: a new therapeutic approach. *Br J Haematol*. 2014;166(2):177-188.
55. de Rooij MF, Kuil A, Geest CR, et al. The clinically active BTK inhibitor PCI-32765 targets B-cell receptor- and chemokine-controlled adhesion and migration in chronic lymphocytic leukemia. *Blood*. 2012;119(11):2590-2594.
56. Tai YT, Chang BY, Kong SY, et al. Bruton tyrosine kinase inhibition is a novel therapeutic strategy targeting tumor in the bone marrow microenvironment in multiple myeloma. *Blood*. 2012;120(9):1877-1887.
57. Chang BY, Francesco M, De Rooij MF, et al. Egress of CD19(+)CD5(+) cells into peripheral blood following treatment with the Bruton tyrosine kinase inhibitor ibrutinib in mantle cell lymphoma patients. *Blood*. 2013;122(14):2412-2424.
58. Anbazhagan K, Rabbind Singh A, Isabelle P, et al. Human pre-B cell receptor signal transduction: evidence for distinct roles of PI3kinase and MAP-kinase signalling pathways. *Immun Inflamm Dis*. 2013;1(1):26-36.